

# MARS: Mesh AutoRegressive Model for 3D Shape Detailization

JINGNAN GAO\*, Shanghai Jiao Tong University, China  
 WEIZHE LIU†, Tencent XR Vision Labs, China  
 WEIXUAN SUN, Tencent XR Vision Labs, China  
 SENBO WANG, Tencent XR Vision Labs, China  
 XIBIN SONG, Tencent XR Vision Labs, China  
 TAIZHANG SHANG, Tencent XR Vision Labs, China  
 SHENZHOU CHEN, Tencent XR Vision Labs, China  
 HONGDONG LI, Australian National University, Australia  
 XIAOKANG YANG, Shanghai Jiao Tong University, China  
 YICHAO YAN‡, Shanghai Jiao Tong University, China  
 PAN JI, Tencent XR Vision Labs, China



Fig. 1. A variety of objects generated by MARS. The figure exemplifies the capability of MARS to generate intricate geometric patterns while preserving the overall shape integrity.

State-of-the-art methods for mesh detailization predominantly utilize Generative Adversarial Networks (GANs) to generate detailed meshes from coarse ones. These methods typically learn a specific style code for each category or similar categories without enforcing geometry supervision across different Levels of Detail (LODs). Consequently, such methods often fail to generalize across a broader range of categories and cannot ensure shape consistency throughout the detailization process. In this paper, we introduce MARS, a novel approach for 3D shape detailization. Our method capitalizes on a novel multi-LOD, multi-category mesh representation to learn shape-consistent mesh representations in latent space across different LODs. We further propose a mesh autoregressive model capable of generating such latent representations through next-LOD token prediction. This approach significantly enhances the realism of the generated shapes. Extensive experiments conducted on the challenging 3D Shape Detailization benchmark demonstrate that our proposed MARS model achieves state-of-the-art performance, surpassing existing methods in both qualitative and quantitative

assessments. Notably, the model’s capability to generate fine-grained details while preserving the overall shape integrity is particularly commendable.

CCS Concepts: • **Computing methodologies** → **Shape modeling**.

Additional Key Words and Phrases: Generative model, geometry detailization, autoregressive model, machine learning.

## 1 INTRODUCTION

With the rapid advancements in generative AI, 3D content has become increasingly prevalent and accessible. Recent developments in deep generative models, particularly those utilizing diffusion processes and vision-language architectures, have significantly enhanced both the accessibility and innovation of generated content. However, while these models excel at producing coarse content efficiently, they often fall short in generating high-quality geometric details. To overcome this limitation and create visually appealing 3D content with intricate geometry, some approaches have focused on scaling up models by training on larger datasets that encompass

\*The contribution is made during an internship at Tencent XR Vision Labs.

†Project lead.

‡Corresponding author.

detailed geometric shapes. This strategy aims to push the boundaries of 3D content generation, ensuring that the resulting outputs are not only accessible but also rich in geometric detail and visual fidelity.

Nevertheless, directly generating shapes with the desired geometric details remains a formidable challenge, as it requires the generative model to grasp the intricate spatial structure of the shape, a task that is difficult to achieve without mesh supervision. Furthermore, in many real-world applications, obtaining a coarse shape is relatively straightforward, either by creating simple polygons or by utilizing similar templates from existing datasets. As a result, training a shape detailization model that transforms a coarse shape into a refined, detailed one emerges as a promising alternative for advancing 3D content generation.

Existing detailization methods predominantly employ Generative Adversarial Networks (GANs) to capture geometric details for shape refinement. These methods typically adhere to the Pyramid GAN structure, assigning different geometric details to various style codes. However, these style codes can only be effectively learned using datasets within similar categories (e.g., Chair and Desk). Consequently, constrained by the generalization capability of the style codes, previous detailization methods can only learn a limited range of styles and fail to fully utilize the available 3D data. This limitation hampers their ability to generalize across diverse categories and leverage the richness of existing 3D datasets, thereby restricting the scope and versatility of the generated geometric details.

To fulfill the task of 3D detailization while leveraging the wealth of available high-quality 3D data, we propose harnessing the power of 3D native generative models. Existing 3D native generative models predominantly rely on the diffusion transformer (DiT) structure for end-to-end generation. Consequently, applying coarse-to-fine techniques for detailization necessitates training multiple DiTs at different resolutions. This architecture demands substantial computational resources and meticulous structural design. In contrast, inspired by recent research in visual autoregressive models (VAR), our method employs an autoregressive model as the 3D shape detailization framework. Specifically, we encode mesh in different levels of detail (LODs) to different tokens, allowing a coarse shape to be interpreted as coarse-LOD tokens, while a fine shape corresponds to fine-LOD tokens. Through autoregressive generation, we achieve detailization by predicting next-LOD tokens given the coarse tokens as a condition.

Our mesh autoregressive model differs from 2D ones in two aspects: 1) 3D data necessitate a distinct encoding-decoding process compared to visual models. 2) The previous end-to-end supervision approach is inadequate for the task of detailization, as tokens of different scales fail to accurately perceive the level-of-detail information and maintain consistency across shapes at various scales. These aspects are crucial for the 3D generation task. Addressing these challenges is essential to ensure that the model can effectively capture and reproduce the intricate geometric details required for high-quality 3D shape detailization. To address these issues, we introduce MARS, a Mesh AutoRegressive model for 3D Shape detailization. Our approach begins with a 3D shape encoding-decoding pipeline to train a multi-LOD, multi-category generative model.

More specifically, we employ a 3D VQVAE with point cloud embedding to compress the mesh into compact tokens. During the training process, we design a geometry-consistency supervision technique to ensure that the tokens capture the geometry information across different levels of detail. This technique enables the model to learn the correspondence between multi-LOD tokens and meshes with different detailization levels. Following the multi-LOD 3D VQVAE, a sequence of discrete tokens is generated, which serves as the coarse-LOD input for the autoregressive model. MARS then accomplishes 3D shape detailization by predicting fine-LOD mesh tokens through next-LOD mesh token generation. Leveraging the capabilities of mesh autoregressive models, our method efficiently generates fine geometric details for various shape inputs while maintaining shape-consistency. Extensive experiments demonstrate the effectiveness of MARS in enhancing 3D shape detailization, showcasing its ability to produce intricate and high-quality geometric details.

To the best of our knowledge, MARS is the first method to leverage an autoregressive model for 3D shape detailization via next-LOD mesh token prediction. In summary, our proposed framework, MARS:

- (1) Proposes a multi-LOD, multi-category 3D VQVAE network with 3D shape encoding-decoding to tokenize shapes into multi-LOD mesh tokens.
- (2) Introduces a geometry-consistency supervision technique to enable the generative model to capture detailed geometric information across different levels of detail.
- (3) Efficiently accomplishes high-quality 3D shape detailization through next-LOD mesh token prediction, achieving state-of-the-art performance across various benchmark settings.

MARS represents a significant advancement in the field of 3D shape detailization, providing a robust and efficient solution for capturing and generating intricate geometric details.

## 2 RELATED WORK

Our work is closely aligned with the domain of 3D generative models, specifically focusing on the intricate task of 3D shape detailization. Additionally, we delve into the realm of autoregressive models, as our method harnesses their capabilities to achieve high-fidelity mesh detailization.

**3D generative models.** Capitalizing on the capabilities of variational autoencoders (VAEs) [Kingma and Welling 2014; van den Oord et al. 2017], generative adversarial networks (GANs) [Goodfellow et al. 2020], autoregressive models [Salimans et al. 2017; van den Oord et al. 2016], and diffusion probabilistic models [Ho et al. 2020; Sohl-Dickstein et al. 2015; Song et al. 2021], a plethora of 3D generative models have been proposed for the generation of 3D shapes. These sophisticated deep generative models utilize voxels [Choy et al. 2016; Hane et al. 2017; Ren et al. 2024; Wu et al. 2016], point clouds [Achlioptas et al. 2018; Fan et al. 2017; Li et al. 2024; Yin et al. 2019; Zeng et al. 2022], neural radiance fields [Hong et al. 2024b; Lin et al. 2023; Mildenhall et al. 2020; Poole et al. 2023; Tang et al. 2024a,b], or neural implicit representations [Chen et al. 2023a; Chen and Zhang 2019; Cui et al. 2024; Gao et al. 2022; Groueix et al. 2018; Hui et al. 2022; Li et al. 2023; Mescheder et al. 2019; Park et al. 2019; Wang et al. 2018; Zhang et al. 2023, 2021] to model 3D

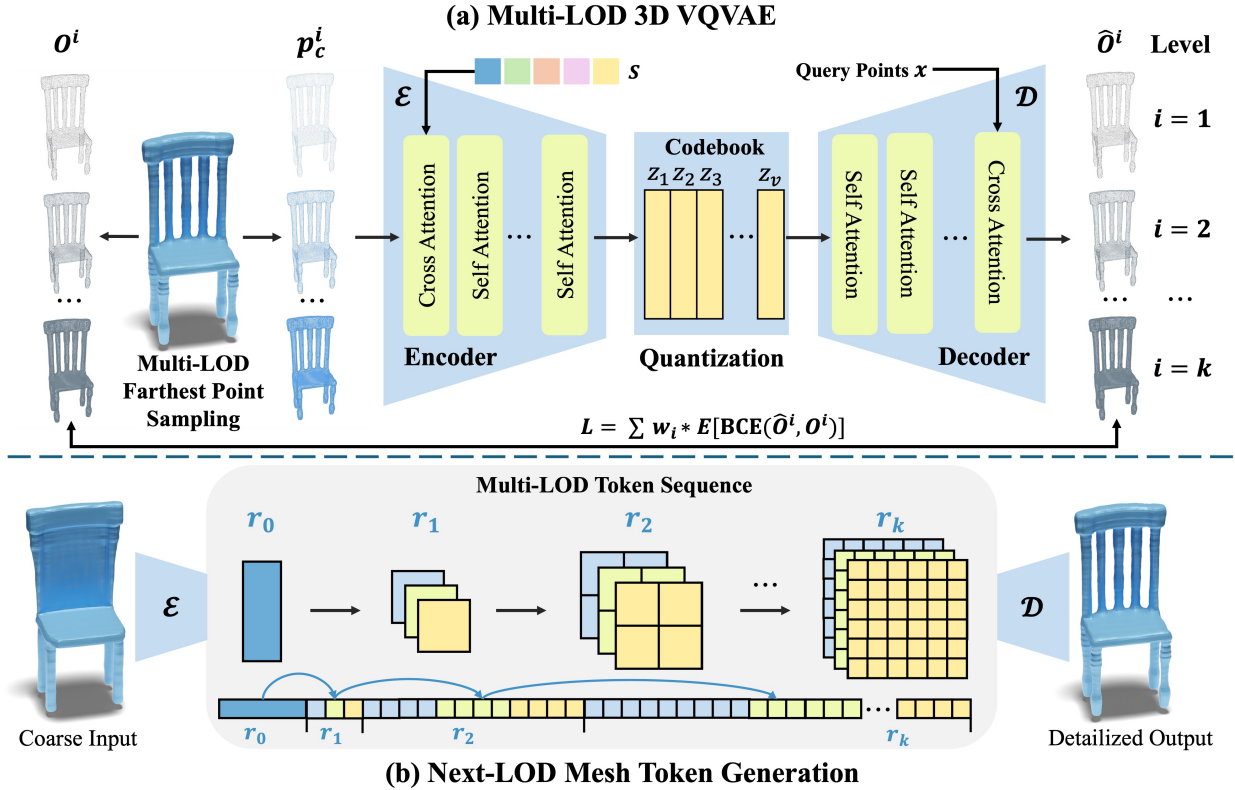


Fig. 2. **Overview of MARS.** Our method initially employs a multi-LOD 3D Vector Quantized Variational Autoencoder (VQVAE) to tokenize input 3D meshes into discrete tokens representing multiple levels of detail. To effectively capture the geometric information across these varying levels, we have devised a geometry-consistency supervision strategy that enhances the training of the VQVAE. For the task of 3D shape detailization, we integrate a mesh autoregressive model that predicts next-LOD mesh tokens. Consequently, our model generates a detailed output that exhibits high-quality geometric details from a coarse input, thereby achieving sophisticated detail enhancement while maintaining structural integrity.

shapes. Among these methodologies, several have been developed to facilitate controllable 3D shape generation for modeling applications. For instance, Point-E [Nichol et al. 2022], Shap-E [Jun and Nichol 2023], and One-2-3-45 [Liu et al. 2023] are capable of generating a 3D model from text or single-image inputs. Conversely, DECOR-GAN [Chen et al. 2021], ShaDDR [Chen et al. 2023b], and DECOLLAGE [Chen et al. 2024a] have been designed to synthesize intricate 3D shapes from coarse voxel input. Despite the fact that DECOLLAGE [Chen et al. 2024a] facilitates interactive style control during generation, it is constrained by its ability to generate only a limited range of detailization styles and its inability to handle out-of-distribution inputs. In stark contrast, our proposed method harnesses the potential of large data and autoregressive models, thereby enabling the generation of a diverse array of detailization styles with superior details.

**3D shape detailization.** Beyond the generation of 3D shapes from scratch, recent advancements have proposed methodologies for coarse-to-fine shape detailization, synthesizing geometric details in the process. Neural subdivision techniques [Liu et al. 2020; Yin et al. 2021] are designed to learn local geometric features from a reference 3D mesh, subsequently transferring these features to a novel shape.

Mesh differentiable rendering methods [Liu et al. 2018; Michel et al. 2022], on the other hand, generate geometric details conditional on a reference image or text. However, these methods are limited by their inability to modify the coarse mesh topology, thereby constraining the range of synthesized detailization. To mitigate this limitation, mesh quilting [Zhou et al. 2006] adopts a strategy of copying and deforming local patches from a given geometric texture patch to detailize the mesh surface. DECOR-GAN [Chen et al. 2021] utilizes the concept of image-to-image translation to generate detailed shapes from coarse voxels, given a conditioned geometric style. ShaDDR [Chen et al. 2023b] further enhances the quality of geometry by incorporating a 2-level hierarchical GAN. DECOLLAGE [Chen et al. 2024a] extends this by employing local style control for improved detailization quality. While these aforementioned methods support the generation of arbitrary mesh topology, they are confined to learned topology and thus, cannot generalize to diverse shapes. In contrast, MARS capitalizes on autoregressive models for next-LOD mesh token prediction, thereby enabling the detailization of a diverse array of shapes.

**Autoregressive models.** Within the realm of image generation, early autoregressive models [Salimans et al. 2017; van den Oord

et al. 2016] were proposed to generate images as sequences of pixels. VQVAE [van den Oord et al. 2017] and VQGAN [Esser et al. 2021] introduced a strategy to quantize images into discrete tokens and employed a transformer to learn the autoregressive priors. Subsequent methods [Chang et al. 2022; Yu et al. 2024] further enhanced the efficiency of tokenization. RQVAE [Lee et al. 2022a] incorporated multi-scale quantization to improve the quality of reconstruction, while VAR [Tian et al. 2024] proposed next-scale prediction for superior reconstruction and accelerated sampling speed. Concurrently, certain methods [Ramesh et al. 2021; Sun et al. 2024] have endeavored to scale up autoregressive models in the task of text-conditioned image generation. However, the autoregressive approach has not been extensively explored in the field of 3D content generation. Our proposed method bridges this gap between autoregressive models and 3D generative models, achieving state-of-the-art performance in the benchmark for 3D shape detailization.

### 3 METHOD

We commence with a concise review of 3D native generative models and visual autoregressive models (VAR) to establish the foundational context requisite for this research (Section 3.1). To facilitate the detailization of 3D shapes, our framework, MARS, initially adopts a multi-LOD 3D vector-quantized variational autoencoder (VQVAE) (Section 3.2) to encode input 3D models into multi-LOD discrete tokens. Subsequently, an autoregressive model is employed to generate mesh tokens at subsequent LOD settings (Section 3.3). A comprehensive depiction of our methodology is illustrated in Fig. 2.

#### 3.1 Preliminaries

**3D native generative models** With the advent of large-scale 3D datasets [Deitke et al. 2023a,b], recent research has focused on training 3D native generative models directly utilizing these datasets. These methodologies [Hong et al. 2024a; Jun and Nichol 2023; Lan et al. 2024; Li et al. 2024; Wu et al. 2024; Zhang et al. 2023, 2024; Zhao et al. 2023] predominantly employ a Variational Autoencoder (VAE) [Kingma and Welling 2014] to compress 3D data into a compact latent representation and subsequently train latent diffusion models to synthesize such representations in latent space. In recent years, several approaches [Chen et al. 2024b,c; Siddiqui et al. 2024] have been proposed to encode meshes into discrete tokens and learn to generate such token sequences using autoregressive transformers. Our method aligns with these 3D native generative models and employs a multi-LOD VQVAE to efficiently generate discrete tokens for autoregressive mesh generation.

**Visual autoregressive models (VAR)** Previous visual autoregressive models [Esser et al. 2021; Lee et al. 2022b; Yu et al. 2022] have predominantly relied on *next-token* prediction to generate image sequences. To enhance sampling speed and reconstruction quality, VAR [Tian et al. 2024] introduces *next-scale* token prediction for image generation. Given an input image  $I$ , VAR initially encodes it into a feature map  $f$  and quantizes  $f$  into  $K$  multi-scale token maps  $R = (r_1, r_2, \dots, r_K)$ , where  $r_K$  corresponds to the resolution of the input  $f$ . The autoregressive likelihood function is then formulated

as:

$$p(r_1, r_2, \dots, r_K) = \prod_{k=1}^K p(r_k | r_1, r_2, \dots, r_{k-1}), \quad (1)$$

where  $r_k$  represents the token map at scale  $k$ . To facilitate next-scale prediction, VAR incorporates a VQVAE with a multi-scale quantizer  $Q(\cdot)$  to tokenize the input image into multi-scale discrete tokens  $R$ :

$$f = \mathcal{E}(I), \quad R = Q(f), \quad (2)$$

where  $\mathcal{E}(\cdot)$  denotes the image encoder. This quantization process maps  $f$  to a sequence of multi-scale token maps by identifying the nearest code in a codebook  $Z$  containing  $V$  vectors:

$$z_k^{(i,j)} = (\arg \min_{v \in [V]} \|(\text{lookup}(Z, v) - r_k^{(i,j)})\|) \in [V], \quad (3)$$

where  $\text{lookup}(Z, v)$  indicates the retrieval of the  $v$ -th vector from codebook  $Z$ . During the VQVAE training, each  $z_k^{(i,j)}$  accesses  $Z$  to approximate the original feature map  $f$  as  $\hat{f}$ . A new image  $\hat{I}$  is subsequently reconstructed using a decoder  $\mathcal{D}(\cdot)$ :

$$\hat{f} = \text{lookup}(Z, z), \quad \hat{I} = \mathcal{D}(\hat{f}). \quad (4)$$

#### 3.2 Multi-LOD 3D VQVAE with Geometry-Consistency Supervision

As depicted in Fig. 2, our methodology commences by tokenizing a coarse mesh  $m_c$  into a token map, followed by predicting a higher Level of Detail (LOD) token map  $r_d$  using  $r_c$  as prefix. The detailed mesh  $m_d$  is then reconstructed by decoding  $r_d$ . Analogous to visual autoregressive models [Tian et al. 2024], we employ a VQVAE for mesh tokenization. However, the conventional VQVAE architecture from VAR is not directly suitable for the task of detailization due to two primary reasons: **1) Distinct Encoding-Decoding Strategy for 3D Data:** Unlike VAR, which is optimized for 2D images, our approach is a 3D native generative model. This necessitates a specifically tailored encoder-decoder structure to accommodate the unique characteristics of 3D data. **2) Modified Supervision for Detailization:** VAR typically utilizes only the final-scale token for supervision. If applied directly using the original VQVAE structure, this would ensure the generation quality at the final scale but fail to maintain geometric consistency across intermediate scales, rendering it inadequate for comprehensive mesh detailization.

To overcome these challenges, we introduce a multi-LOD 3D VQVAE that incorporates geometry-consistency supervision. Initially, we utilize a 3D shape encoder-decoder framework to capture latent set representations. Subsequently, we integrate geometry-consistency supervision to effectively facilitate the task of detailization. This strategy ensures that each multi-LOD token contributes to the overall fidelity and geometric consistency of the generated meshes, aligning with the specific requirements of 3D data processing and detail enhancement. This approach not only enhances the detail fidelity but also ensures that the structural integrity of the mesh is maintained across different levels of detail.

**3D Shape Encoding-Decoding.** Consistent with the methodologies outlined in [Li et al. 2024; Zhang et al. 2023, 2024], we transform 3D assets into a compact one-dimensional latent set, denoted as  $S = \{s_i \in \mathcal{R}^C\}_{i=1}^D$ . In this notation,  $D$  represents the number of latent sets, and  $C$  indicates the dimensionality of the features within

each set. We adopt an autoencoder architecture to encode 3D shapes into these latent sets. Specifically, for each 3D shape, we sample a set of point clouds, denoted as  $p_c \in \mathcal{R}^{N \times 3}$ , along with their corresponding surface normals  $p_n$  where  $N$  denotes the number of sampling points. We further apply Fourier positional encoding to capture the geometric information and integrate a cross-attention layer to infuse this information into the encoder. To effectively encapsulate geometric features, we utilize a Perceiver-based shape encoder  $\mathcal{E}$ , as proposed in [Li et al. 2024; Zhang et al. 2023], to learn the latent set  $S$ :

$$\begin{aligned} p_f &= \text{PE}(p_c) \oplus p_n, \\ \mathcal{E}(p_c, p_n) &= \mathcal{Q}(\text{SelfAttn}(\text{CrossAttn}(S, p_f))), \end{aligned} \quad (5)$$

where  $\oplus$  denotes concatenation,  $\mathcal{Q}$  represents the quantizer, and  $\text{PE}$  stands for the Fourier positional encoding function. To decode the latent set  $S$ , we employ a Perceiver-based decoder, similar to the one described in [Li et al. 2024], which arranges all self-attention layers prior to the cross-attention layers. The decoder  $\mathcal{D}$  predicts the occupancy value given a query 3D point  $x$  and the shape latent embeddings  $S$ :

$$O(\cdot) = O(\text{CrossAttn}(\text{PE}(x), S)), \quad (6)$$

where  $O(\cdot)$  is the occupancy prediction function using a Multilayer Perceptron (MLP). This architecture facilitates the accurate reconstruction of 3D shapes by leveraging the rich geometric information encoded in the latent sets.

**Geometry-Consistency Supervision.** In the context of our mesh autoregressive models, we represent a detailed mesh as a finer Level of Detail (LOD) token, which is derived from a coarser-LOD token corresponding to the given coarse mesh. To achieve effective 3D shape detailization, our model is designed to capture the correspondence between multi-LOD tokens and meshes across varying levels of detail. Specifically, the prediction of the next-LOD token simulates the progressive mesh detailization process. We facilitate the learning of this pattern within the VQVAE by incorporating geometry-consistency supervision. For each point cloud  $p$  in the training dataset, we initially generate a final-LOD shape through dense sampling and subsequently obtain a coarser-LOD shape via downsampling. To manage geometric details across different LODs while maintaining overall geometric consistency, we utilize farthest point sampling (FPS) as our downsampling strategy. As the number of point clouds changes with each LOD after downsampling, the query 3D point is similarly processed, resulting in  $x^i$  for the  $i$ -th LOD. This variation in point cloud density across LODs leads to latents of differing lengths, initially causing a dimension misalignment since the decoder requires a fixed-length latent input. To resolve this issue without the need for multiple LOD-specific decoders, we standardize the variable-length mesh tokens to a fixed-length sequence:

$$R^i = \text{Pad}(R^i, 0), \quad (7)$$

where we pad the original  $i$ -th LOD mesh token  $R^i$  to the length of  $R^K$ . Following this procedure, we compute the occupancy  $O^i$  for each LOD. This strategy simplifies the architecture by eliminating the need for multiple decoders and ensures that different LOD tokens effectively learn distinct levels of detail. The geometry-consistency supervision is then quantified using the Binary Cross Entropy (BCE)

loss:

$$\mathcal{L}_{vae} = \sum_{i=1}^K w_i \mathbb{E}_{x^i \in \mathcal{R}^3} [\text{BCE}(\hat{O}^i(x^i), O^i)] + \lambda_{vq} \mathcal{L}_{vq}, \quad (8)$$

where  $\hat{O}^i(x^i)$  represents the ground-truth occupancy value of the  $i$ -th LOD 3D point  $x$ ,  $w_i$  denotes the weight for the  $i$ -th LOD,  $K$  is the final LOD number and  $\mathcal{L}_{vq}$  is the commitment loss of the VQVAE following [van den Oord et al. 2017] with weight  $\lambda_{vq}$ . This formulation ensures that our model robustly learns detailed geometric features across multiple LODs, enhancing the fidelity and consistency of the generated 3D meshes.

### 3.3 Next-LOD Mesh Token Generation

Upon training the multi-LOD 3D VQVAE, a sequence of discrete tokens is generated, which then serves as the input for the autoregressive model. To facilitate the prediction of the next-LOD mesh token for 3D shape detailization, we employ an autoregressive (AR) model that utilizes a decoder-only transformer architecture, similar to those used in GPT-2 and VQGAN, and incorporates adaptive normalization (AdaLN). The autoregressive process initiates with a single token and incrementally predicts subsequent, finer LOD tokens, each conditioned on the preceding coarser tokens. To enhance computational efficiency, all tokens  $L^{(s)}$  at LOD  $s$  are generated simultaneously in parallel. During the training phase, a block-wise causal attention mask is employed to ensure that each token only attends to its preceding tokens, thereby preserving the causal structure necessary for the autoregressive model. For the inference phase, we integrate the kv-caching technique [Pope et al. 2023] to expedite the sampling process. This approach not only streamlines the generation of high-fidelity 3D meshes but also ensures that the detailization process is both efficient and scalable.

## 4 EXPERIMENT

### 4.1 Mesh Detailization Comparison

**Qualitative Comparison.** We evaluate our model against state-of-the-art mesh detailization approaches, namely ShaDDR [Chen et al. 2023b] and DECOLLAGE [Chen et al. 2024a], using the benchmark dataset previously described. For a consistent evaluation framework, we adopt the methodology from prior works [Chen et al. 2024a, 2023b], utilizing a template mesh for each category as the input and applying different detailization methods to ensure comparability. Fig. 3 presents qualitative comparisons with these two leading detailization approaches. As illustrated, both ShaDDR and DECOLLAGE exhibit limitations in generating detailed geometry when trained on multi-category data. These methods, which employ GANs for detailization, necessitate training datasets comprised of similar categories due to their reliance on learning category-specific style codes for detailization. Consequently, their inability to generalize across a multi-category dataset restricts their flexibility and applicability. Additionally, these methods often produce damaged mesh parts, further impeding practical applications. In contrast, our approach harnesses the capabilities of the geometry-consistent VQVAE model, adept at representing multi-category meshes across various levels of detail. The 3D autoregressive model we propose effectively generates multi-LOD representations across different

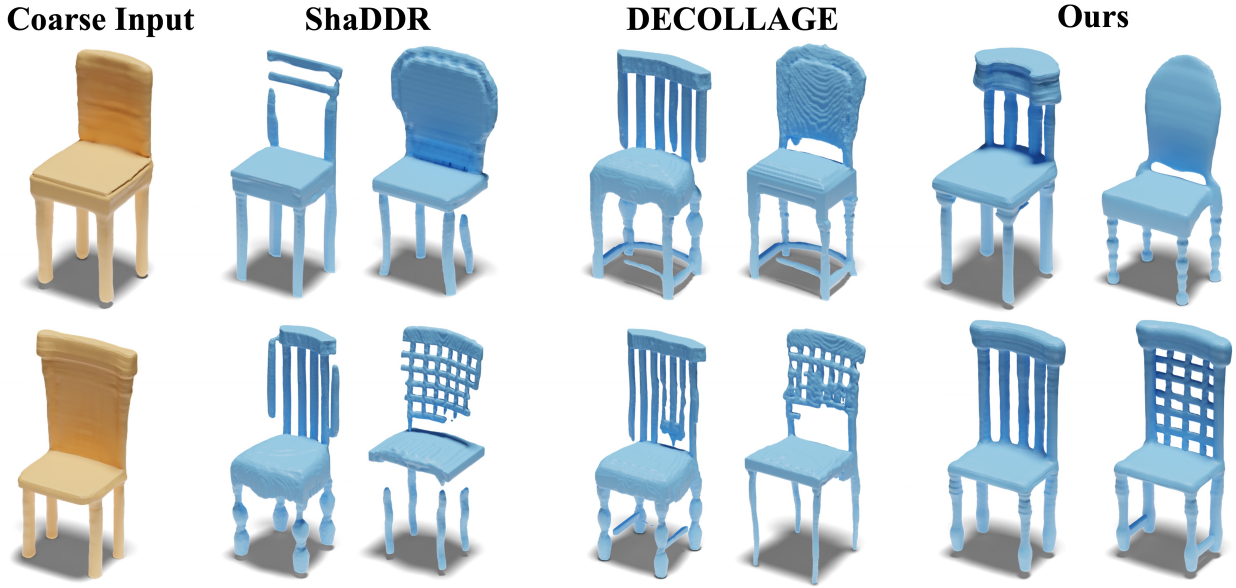


Fig. 3. **Comparison with previous detailization approaches.** We conduct a comparative analysis of our model with existing detailization methods, specifically ShaDDR and DECOLLAGE. For each coarse input, we demonstrate two distinct detailization styles. It is observed that both ShaDDR and DECOLLAGE often produce outputs with compromised mesh integrity. In contrast, our method consistently generates complete outputs that exhibit high-quality geometric details, thereby underscoring the robustness and efficacy of our approach in handling complex detailization tasks.

categories and detail levels, thereby demonstrating superior performance compared to the baseline models. Furthermore, we juxtapose our detailization results with those of ShaDDR and DECOLLAGE trained on similar-category data. As depicted in Fig. 7, our method not only preserves complete shape integrity but also enhances the geometric detail, surpassing previous methods. Additionally, Figs. 4 and 8 showcase the diversity of our generation results. These figures illustrate that our method is capable of producing a variety of detailed outputs from the same coarse input, highlighting the robustness and versatility of our approach in generating diverse and detailed 3D meshes.

**Quantitative Comparison.** To rigorously evaluate the effectiveness of our model, we adopt several quantitative metrics as utilized in prior research. We conduct comparisons of our approach with ShaDDR and DECOLLAGE across both multi-category datasets, which highlight the limitations of baseline models in handling objects with significant variations, and similar-category datasets, denoted as *ShaDDR-S* and *DECOLLAGE-S* in accordance with the literature, to demonstrate the consistent superiority of our model over the baseline approaches. All models are evaluated following the established protocol of DECOLLAGE, and the results are presented in Table 1. To determine the fidelity with which the generated shapes adhere to the structures of the input shapes, we employ the Strict-IOU metric, which quantifies the Intersection over Union (IOU) between the downsampled detailed output and the coarse input. Additionally, we utilize the Loose-IOU metric to calculate the proportion of occupied voxels in the input that correspond to similarly occupied voxels in the downsampled output. Furthermore, we employ the F-Score to assess the similarity between the generated

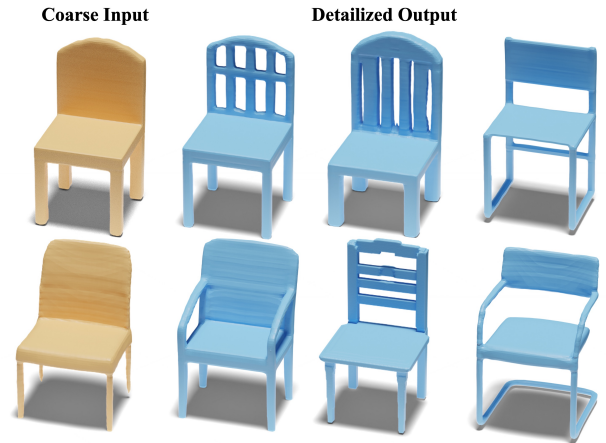


Fig. 4. **Diverse generation results.** Our approach is capable of generating a diverse array of detailed meshes from a uniform coarse input. This capability underscores the robustness and adaptability of our method in enhancing mesh detailization across various scenarios.

results and the coarse input shapes at a local level. A high F-Score indicates that the local details of the generated shapes closely mirror those of the input shapes, thereby enhancing the local plausibility of the generated shapes.

## 4.2 Ablation Study

**Geometry-Consistency Supervision.** Our method integrates geometry-consistency supervision to ensure shape-consistent mesh generation

Method	Strict-IOU $\uparrow$	Loose-IOU $\uparrow$	F-Score $\uparrow$
ShaDDR	0.512	0.668	0.898
ShaDDR-S	0.596	0.760	0.907
DECOLLAGE	0.627	0.791	0.901
DECOLLAGE-S	0.748	0.908	0.914
Ours	<b>0.785</b>	<b>0.924</b>	<b>0.918</b>

Table 1. **Quantitative comparison of different detailization methods.** Our approach consistently surpasses previous methodologies across all evaluation metrics, within both multi-category and similar-category settings. For clarity, ShaDDR and DECOLLAGE when applied to similar-category datasets are referred to as *ShaDDR-S* and *DECOLLAGE-S*, respectively.



Fig. 5. **Reconstruction ablation of geometry-consistency supervision.** It can be seen that the geometry-consistency supervision is crucial in our shape detailization process.

across varying levels of detail. The efficacy of this supervision is demonstrated through the presentation of ablation reconstruction results in Fig. 5. Our model facilitates detailization by initially representing the coarse mesh input as a coarse token, followed by the prediction of subsequent level-of-detail (LOD) mesh tokens. The geometry-consistency supervision acts as a directive for LOD guidance within the mesh token framework. As evidenced, the incorporation of geometry-consistency supervision enables our model to incrementally learn the detailization process. In contrast, the absence of geometry-consistency supervision results in the reconstruction of compromised geometries, as the model struggles to interpret the LOD nuances associated with different mesh tokens.

**VQVAE Codebook Size.** During the training of the VQVAE, the size of the codebook significantly influences the quality of the reconstruction results. We conduct ablation studies by varying the codebook size  $V$  to 4096, 8192, and 16384. The comparative results are illustrated in Fig. 6. To quantitatively evaluate the reconstruction quality, we measure the accuracy of the recovered occupancy and the corresponding Intersection Over Union (IOU) derived from the latents on a subset of our constructed dataset. These results are detailed in Table 2. Our method achieves comparable performance when utilizing codebook sizes of 8192 and 16384, which are superior to the results obtained with a codebook size of 4096.

**Downsampling Strategy.** By incorporating a geometry-consistency supervision loss, our method effectively captures geometric information across various levels of detail. During training, we downsample

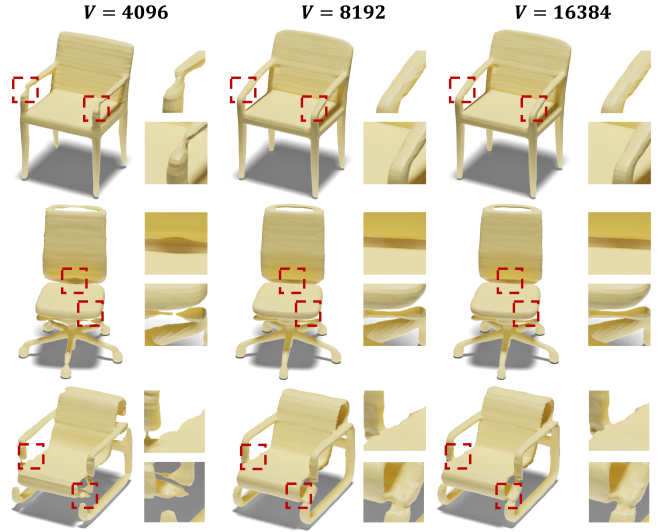


Fig. 6. **Comparison of reconstruction using different codebook sizes.** It is apparent that our method yields comparable outcomes when employing codebook sizes of 8192 and 16384, with these results surpassing those obtained using a codebook size of 4096.

Codebook Size $V$	4096	8192	16384
Accuracy	0.902	0.964	0.972
IOU	0.874	0.904	0.916

Table 2. **Quantitative comparison of different codebook sizes  $V$ .** The results demonstrate that utilizing a codebook size of 8192 yields superior outcomes compared to a size of 4096, and achieves results that are comparable to those obtained with a codebook size of 16384.

the point clouds to create a dataset that encompasses different levels of geometric detail. The farthest point sampling (FPS) strategy is utilized for downsampling. We conduct an ablation study to compare the efficacy of the FPS strategy with that of uniform sampling. The results, including mid-Level of Detail (LOD) reconstructions using each sampling strategy and the final-LOD reconstruction as a reference, are presented. As illustrated in Fig. 9, our model, when employing FPS, more effectively captures the level-of-detail information. This effectiveness is attributed to the FPS’s tendency to preserve the overall shape of the geometry during downsampling. Consequently, each downsampling step primarily reduces high-frequency geometric details while retaining the structural integrity of the shape. The model subsequently learns to incrementally refine the geometric details in a reverse manner.

### 4.3 Applications

Our model enhances a coarse shape by tokenizing it into mesh tokens and predicting the next Level of Detail (LOD) mesh tokens. Consequently, our approach is capable of constructing meshes with varying levels of detail, as depicted in Fig. 10. We further evaluate our model on an out-of-distribution object (a house from ShaDDR [Chen et al. 2023b]) and provide a comparison with an in-distribution shape

condition (a car from ShapeNet [Chang et al. 2015]). The results, illustrated in Fig. 11, demonstrate that our method effectively generates a house in the form of a car. This application underscores our model’s ability to capture geometric features and generate high-quality details while maintaining the overall shape integrity. Additionally, we present the results of texturing the refined shape in Fig. 12. Given that our model processes a coarse mesh and outputs a detailed mesh, it can serve as a valuable tool for mesh refinement within the 3D generation pipeline, offering an efficient and robust method for capturing and rendering intricate geometric details.

## 5 CONCLUSION

In this work, we introduce MARS, a mesh autoregressive model designed for 3D shape refinement. Our method leverages the capabilities of autoregressive models to generate high-fidelity geometric details. MARS is founded on two principal components: 1) A multi-Level of Detail (LOD) 3D Vector Quantized Variational Autoencoder (VQVAE) that encodes and decodes 3D shapes into multi-LOD mesh tokens, and 2) An autoregressive mechanism for predicting next-LOD mesh tokens, facilitating high-quality 3D shape refinement. Extensive experiments validate that our approach not only achieves high-quality refinement but also preserves the overall shape integrity. Our model sets a new benchmark in the domain of 3D shape refinement, demonstrating state-of-the-art performance and marking a significant advancement in the field.

## REFERENCES

- Panos Achlioptas, Olga Diamanti, Ioannis Mitliagkas, and Leonidas J. Guibas. 2018. Learning Representations and Generative Models for 3D Point Clouds. In *ICML*, Vol. 80. 40–49.
- Angel X. Chang, Thomas Funkhouser, Leonidas Guibas, Pat Hanrahan, Qixing Huang, Zimo Li, Silvio Savarese, Manolis Savva, Shuran Song, Hao Su, Jianxiong Xiao, Li Yi, and Fisher Yu. 2015. ShapeNet: An Information-Rich 3D Model Repository. *arXiv preprint arXiv:1512.03012* (2015).
- Huiwen Chang, Han Zhang, Lu Jiang, Ce Liu, and William T. Freeman. 2022. MaskGIT: Masked Generative Image Transformer. In *CVPR*. 11305–11315.
- Qimin Chen, Zhiqin Chen, Vladimir G. Kim, Noam Aigerman, Hao (Richard) Zhang, and Siddhartha Chaudhuri. 2024a. DECOLLAGE: 3D Detailization by Controllable, Localized, and Learned Geometry Enhancement. In *ECCV*, Vol. 15097. 110–127.
- Qimin Chen, Zhiqin Chen, Hang Zhou, and Hao Zhang. 2023b. ShaDDR: Interactive Example-Based Geometry and Texture Generation via 3D Shape Detailization and Differentiable Rendering. In *SIGGRAPH Asia*. ACM, 58:1–58:11.
- Rui Chen, Yongwei Chen, Ningxin Jiao, and Kui Jia. 2023a. Fantasia3D: Disentangling Geometry and Appearance for High-quality Text-to-3D Content Creation. In *ICCV*. 22189–22199.
- Yiwen Chen, Tong He, Di Huang, Weicai Ye, Sijin Chen, Jiayang Tang, Xin Chen, Zhong-gang Cai, Lei Yang, Gang Yu, Guosheng Lin, and Chi Zhang. 2024b. MeshAnything: Artist-Created Mesh Generation with Autoregressive Transformers. *arXiv preprint arXiv:2406.10163* (2024).
- Yiwen Chen, Yikai Wang, Yihao Luo, Zhengyi Wang, Zilong Chen, Jun Zhu, Chi Zhang, and Guosheng Lin. 2024c. MeshAnything V2: Artist-Created Mesh Generation With Adjacent Mesh Tokenization. *arXiv preprint arXiv:2408.02555* (2024).
- Zhiqin Chen, Vladimir G. Kim, Matthew Fisher, Noam Aigerman, Hao Zhang, and Siddhartha Chaudhuri. 2021. DECOR-GAN: 3D Shape Detailization by Conditional Refinement. In *CVPR*. 15740–15749.
- Zhiqin Chen and Hao Zhang. 2019. Learning Implicit Fields for Generative Shape Modeling. In *CVPR*. 5939–5948.
- Christopher B. Choy, Danfei Xu, JunYoung Gwak, Kevin Chen, and Silvio Savarese. 2016. 3D-R2N2: A Unified Approach for Single and Multi-view 3D Object Reconstruction. In *ECCV*, Vol. 9912. 628–644.
- Ruikai Cui, Weizhe Liu, Weixuan Sun, Senbo Wang, Taizhang Shang, Yang Li, Xibin Song, Han Yan, Zhennan Wu, Shenzhou Chen, Hongdong Li, and Ji Pan. 2024. Neusdiffusion: A spatial-aware generative model for 3d shape completion, reconstruction, and generation. In *ECCV*.
- Matt Deitke, Ruoshi Liu, Matthew Wallingford, Huong Ngo, Oscar Michel, Aditya Kusupati, Alan Fan, Christian Laforte, Vikram Voleti, Samir Yitzhak Gadre, Eli VanderBilt, Aniruddha Kembhavi, Carl Vondrick, Georgia Gkioxari, Kiana Ehsani, Ludwig Schmidt, and Ali Farhadi. 2023a. Objaverse-XL: A Universe of 10M+ 3D Objects. In *NeurIPS*.
- Matt Deitke, Dustin Schwenk, Jordi Salvador, Luca Weihs, Oscar Michel, Eli VanderBilt, Ludwig Schmidt, Kiana Ehsani, Aniruddha Kembhavi, and Ali Farhadi. 2023b. Objaverse: A Universe of Annotated 3D Objects. In *CVPR*. 13142–13153.
- Patrick Esser, Robin Rombach, and Björn Ommer. 2021. Taming Transformers for High-Resolution Image Synthesis. In *CVPR*. 12873–12883.
- Haoqiang Fan, Hao Su, and Leonidas J. Guibas. 2017. A Point Set Generation Network for 3D Object Reconstruction from a Single Image. In *CVPR*. 2463–2471.
- Jun Gao, Tianchang Shen, Zian Wang, Wenzheng Chen, Kangxue Yin, Daiqing Li, Or Litany, Zan Gojcic, and Sanja Fidler. 2022. GET3D: A Generative Model of High Quality 3D Textured Shapes Learned from Images. In *NeurIPS*.
- Ian J. Goodfellow, Jean Pouget-Abadie, Mehdi Mirza, Bing Xu, David Warde-Farley, Sherjil Ozair, Aaron C. Courville, and Yoshua Bengio. 2020. Generative adversarial networks. *Commun. ACM* 63, 11 (2020), 139–144.
- Thibault Groueix, Matthew Fisher, Vladimir G. Kim, Bryan C. Russell, and Mathieu Aubry. 2018. A Papier-Mâché Approach to Learning 3D Surface Generation. In *CVPR*. 216–224.
- Christian Hane, Shubham Tulsiani, and Jitendra Malik. 2017. Hierarchical Surface Prediction for 3D Object Reconstruction. In *3DV*. 412–420.
- Jonathan Ho, Ajay Jain, and Pieter Abbeel. 2020. Denoising Diffusion Probabilistic Models. In *NeurIPS*.
- Fangzhou Hong, Jiayang Tang, Ziang Cao, Min Shi, Tong Wu, Zhaoxi Chen, Tengfei Wang, Liang Pan, Dahua Lin, and Ziwei Liu. 2024a. 3DTopia: Large Text-to-3D Generation Model with Hybrid Diffusion Priors. *arXiv preprint arXiv:2403.02234* (2024).
- Yicong Hong, Kai Zhang, Jiuxiang Gu, Sai Bi, Yang Zhou, Difan Liu, Feng Liu, Kalyan Sunkavalli, Trung Bui, and Hao Tan. 2024b. LRM: Large Reconstruction Model for Single Image to 3D. In *ICLR*.
- Ka-Hei Hui, Ruihui Li, Jingyu Hu, and Chi-Wing Fu. 2022. Neural Wavelet-domain Diffusion for 3D Shape Generation. In *SIGGRAPH Asia*. 24:1–24:9.
- Heewoo Jun and Alex Nichol. 2023. Shap-E: Generating Conditional 3D Implicit Functions. *arXiv preprint arXiv:2305.02463* (2023).
- Diederik P. Kingma and Max Welling. 2014. Auto-Encoding Variational Bayes. In *ICLR*.

- Yushi Lan, Fangzhou Hong, Shuai Yang, Shangchen Zhou, Xuyi Meng, Bo Dai, Xingang Pan, and Chen Change Loy. 2024. LN3Diff: Scalable Latent Neural Fields Diffusion for Speedy 3D Generation. In *ECCV*, Vol. 15062. 112–130.
- Doyup Lee, Chiheon Kim, Saehoon Kim, Minsu Cho, and Wook-Shin Han. 2022a. Autoregressive Image Generation using Residual Quantization. In *CVPR*. 11513–11522.
- Doyup Lee, Chiheon Kim, Saehoon Kim, Minsu Cho, and Wook-Shin Han. 2022b. Autoregressive Image Generation using Residual Quantization. In *CVPR*. 11513–11522.
- Muheng Li, Yueqi Duan, Jie Zhou, and Jiwen Lu. 2023. Diffusion-SDF: Text-to-Shape via Voxelized Diffusion. In *CVPR*. 12642–12651.
- Weiyu Li, Jiarui Liu, Rui Chen, Yixun Liang, Xuelin Chen, Ping Tan, and Xiaoxiao Long. 2024. CraftsMan: High-fidelity Mesh Generation with 3D Native Generation and Interactive Geometry Refiner. *arXiv preprint arXiv:2405.14979* (2024).
- Chen-Hsuan Lin, Jun Gao, Luming Tang, Towaki Takikawa, Xiao-hui Zeng, Xun Huang, Karsten Kreis, Sanja Fidler, Ming-Yu Liu, and Tsung-Yi Lin. 2023. Magic3D: High-Resolution Text-to-3D Content Creation. In *CVPR*. 300–309.
- Hsueh-Ti Derek Liu, Vladimir G. Kim, Siddhartha Chaudhuri, Noam Aigerman, and Alec Jacobson. 2020. Neural subdivision. *ACM Trans. Graph.* 39, 4 (2020), 124.
- Hsueh-Ti Derek Liu, Michael Tao, and Alec Jacobson. 2018. Paparazzi: surface editing by way of multi-view image processing. *ACM Trans. Graph.* 37, 6 (2018), 221.
- Minghua Liu, Chao Xu, Haiyan Jin, Linghao Chen, Mukund Varma T., Zexiang Xu, and Hao Su. 2023. One-2-3-45: Any Single Image to 3D Mesh in 45 Seconds without Per-Shape Optimization. In *NeurIPS*.
- Lars M. Mescheder, Michael Oechsle, Michael Niemeyer, Sebastian Nowozin, and Andreas Geiger. 2019. Occupancy Networks: Learning 3D Reconstruction in Function Space. In *CVPR*. 4460–4470.
- Oscar Michel, Roi Bar-On, Richard Liu, Sagie Benaim, and Rana Hanocka. 2022. Text2Mesh: Text-Driven Neural Stylization for Meshes. In *CVPR*. 13482–13492.
- Ben Mildenhall, Pratul P. Srinivasan, Matthew Tancik, Jonathan T. Barron, Ravi Ramamoorthi, and Ren Ng. 2020. NeRF: Representing Scenes as Neural Radiance Fields for View Synthesis. In *ECCV*, Vol. 12346. 405–421.
- Alex Nichol, Heewoo Jun, Prafulla Dhariwal, Pamela Mishkin, and Mark Chen. 2022. Point-E: A System for Generating 3D Point Clouds from Complex Prompts. *arXiv preprint arXiv:2212.08751* (2022).
- Jeong Joon Park, Peter R. Florence, Julian Straub, Richard A. Newcombe, and Steven Lovegrove. 2019. DeepSDF: Learning Continuous Signed Distance Functions for Shape Representation. In *CVPR*. 165–174.
- Ben Poole, Ajay Jain, Jonathan T. Barron, and Ben Mildenhall. 2023. DreamFusion: Text-to-3D using 2D Diffusion. In *ICLR*.
- Reiner Pope, Sholto Douglas, Aakanksha Chowdhery, Jacob Devlin, James Bradbury, Jonathan Heek, Kefan Xiao, Shivani Agrawal, and Jeff Dean. 2023. Efficiently Scaling Transformer Inference. In *Proceedings of Machine Learning and Systems*.
- Aditya Ramesh, Mikhail Pavlov, Gabriel Goh, Scott Gray, Chelsea Voss, Alec Radford, Mark Chen, and Ilya Sutskever. 2021. Zero-Shot Text-to-Image Generation. In *ICML*, Vol. 139. 8821–8831.
- Xuanchi Ren, Jiahui Huang, Xiaohui Zeng, Ken Museth, Sanja Fidler, and Francis Williams. 2024. XCube: Large-Scale 3D Generative Modeling using Sparse Voxel Hierarchies. In *CVPR*. 4209–4219.
- Tim Salimans, Andrej Karpathy, Xi Chen, and Diederik P. Kingma. 2017. PixelCNN++: Improving the PixelCNN with Discretized Logistic Mixture Likelihood and Other Modifications. In *ICLR*.
- Yawar Siddiqui, Antonio Alliegro, Alexey Artemov, Tatiana Tommasi, Daniele Sirigatti, Vladislav Rosov, Angela Dai, and Matthias Nießner. 2024. MeshGPT: Generating Triangle Meshes with Decoder-Only Transformers. In *CVPR*. 19615–19625.
- Jascha Sohl-Dickstein, Eric A. Weiss, Niru Maheswaranathan, and Surya Ganguli. 2015. Deep Unsupervised Learning using Nonequilibrium Thermodynamics. In *ICML*, Vol. 37. 2256–2265.
- Yang Song, Jascha Sohl-Dickstein, Diederik P. Kingma, Abhishek Kumar, Stefano Ermon, and Ben Poole. 2021. Score-Based Generative Modeling through Stochastic Differential Equations. In *ICLR*.
- Peize Sun, Yi Jiang, Shoufa Chen, Shilong Zhang, Bingyue Peng, Ping Luo, and Zehuan Yuan. 2024. Autoregressive Model Beats Diffusion: Llama for Scalable Image Generation. *arXiv preprint arXiv:2406.06525* (2024).
- Jiaxiang Tang, Zhaoxi Chen, Xiaokang Chen, Tengfei Wang, Gang Zeng, and Ziwei Liu. 2024a. LGM: Large Multi-view Gaussian Model for High-Resolution 3D Content Creation. In *ECCV*, Vol. 15062. 1–18.
- Jiaxiang Tang, Jiawei Ren, Hang Zhou, Ziwei Liu, and Gang Zeng. 2024b. DreamGaussian: Generative Gaussian Splatting for Efficient 3D Content Creation. In *ICLR*.
- Keyu Tian, Yi Jiang, Zehuan Yuan, Bingyue Peng, and Liwei Wang. 2024. Visual Autoregressive Modeling: Scalable Image Generation via Next-Scale Prediction. In *NeurIPS*.
- Aäron van den Oord, Nal Kalchbrenner, Lasse Espeholt, Koray Kavukcuoglu, Oriol Vinyals, and Alex Graves. 2016. Conditional Image Generation with PixelCNN Decoders. In *NeurIPS*. 4790–4798.
- Aäron van den Oord, Oriol Vinyals, and Koray Kavukcuoglu. 2017. Neural Discrete Representation Learning. In *NeurIPS*. 6306–6315.
- Nanyang Wang, Yinda Zhang, Zhuwen Li, Yanwei Fu, Wei Liu, and Yu-Gang Jiang. 2018. Pixel2Mesh: Generating 3D Mesh Models from Single RGB Images. In *ECCV*, Vol. 11215. 55–71.
- Jiajun Wu, Chengkai Zhang, Tianfan Xue, Bill Freeman, and Josh Tenenbaum. 2016. Learning a Probabilistic Latent Space of Object Shapes via 3D Generative-Adversarial Modeling. In *NeurIPS*. 82–90.
- Shuang Wu, Youtian Lin, Feihu Zhang, Yifei Zeng, Jingxi Xu, Philip Torr, Xun Cao, and Yao Yao. 2024. Direct3D: Scalable Image-to-3D Generation via 3D Latent Diffusion Transformer. In *NeurIPS*.
- Kangxue Yin, Zhiqin Chen, Hui Huang, Daniel Cohen-Or, and Hao Zhang. 2019. LOGAN: unpaired shape transform in latent overcomplete space. *ACM Trans. Graph.* 38, 6 (2019), 198:1–198:13.
- Kangxue Yin, Jun Gao, Maria Shugrina, Sameh Khamis, and Sanja Fidler. 2021. 3DStyleNet: Creating 3D Shapes with Geometric and Texture Style Variations. In *ICCV*. 12436–12445.
- Jiahui Yu, Xin Li, Jing Yu Koh, Han Zhang, Ruoming Pang, James Qin, Alexander Ku, Yuanzhong Xu, Jason Baldridge, and Yonghui Wu. 2022. Vector-quantized Image Modeling with Improved VQGAN. In *ICLR*.
- Qihang Yu, Mark Weber, Xueqing Deng, Xiaohui Shen, Daniel Cremers, and Liang-Chieh Chen. 2024. An Image is Worth 32 Tokens for Reconstruction and Generation. In *NeurIPS*.
- Xiaohui Zeng, Arash Vahdat, Francis Williams, Zan Gojic, Or Litany, Sanja Fidler, and Karsten Kreis. 2022. LION: Latent Point Diffusion Models for 3D Shape Generation. In *NeurIPS*.
- Biao Zhang, Jiapeng Tang, Matthias Nießner, and Peter Wonka. 2023. 3DShape2VecSet: A 3D Shape Representation for Neural Fields and Generative Diffusion Models. *ACM Trans. Graph.* 42, 4 (2023), 92:1–92:16.
- Longwen Zhang, Ziyu Wang, Qixuan Zhang, Qiwei Qiu, Anqi Pang, Haoran Jiang, Wei Yang, Lan Xu, and Jingyi Yu. 2024. CLAY: A Controllable Large-scale Generative Model for Creating High-quality 3D Assets. *ACM Trans. Graph.* 43, 4 (2024), 120:1–120:20.
- Yuxuan Zhang, Wenzheng Chen, Huan Ling, Jun Gao, Yinan Zhang, Antonio Torralba, and Sanja Fidler. 2021. Image GANs meet Differentiable Rendering for Inverse Graphics and Interpretable 3D Neural Rendering. In *ICLR*.
- Zibo Zhao, Wen Liu, Xin Chen, Xianfang Zeng, Rui Wang, Pei Cheng, Bin Fu, Tao Chen, Gang Yu, and Shenghua Gao. 2023. Michelangelo: Conditional 3D Shape Generation based on Shape-Image-Text Aligned Latent Representation. In *NeurIPS*.
- Kun Zhou, Xin Huang, Xi Wang, Yiyang Tong, Mathieu Desbrun, Baining Guo, and Heung-Yeung Shum. 2006. Mesh quilting for geometric texture synthesis. *ACM Trans. Graph.* 25, 3 (2006), 690–697.

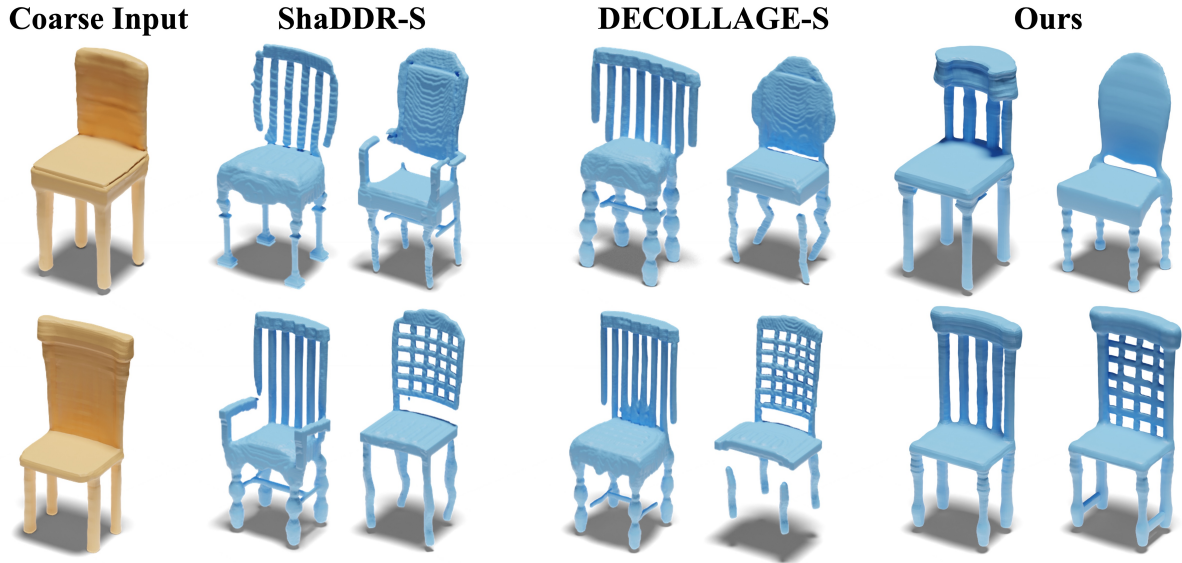


Fig. 7. **Comparison with previous detailization methods.** We evaluate our model by comparing it with the original ShaDDR and DECOLLAGE, both trained using datasets from similar categories. For each coarse input, we present two distinct detailization styles, demonstrating the versatility and adaptability of our approach in generating refined outputs.

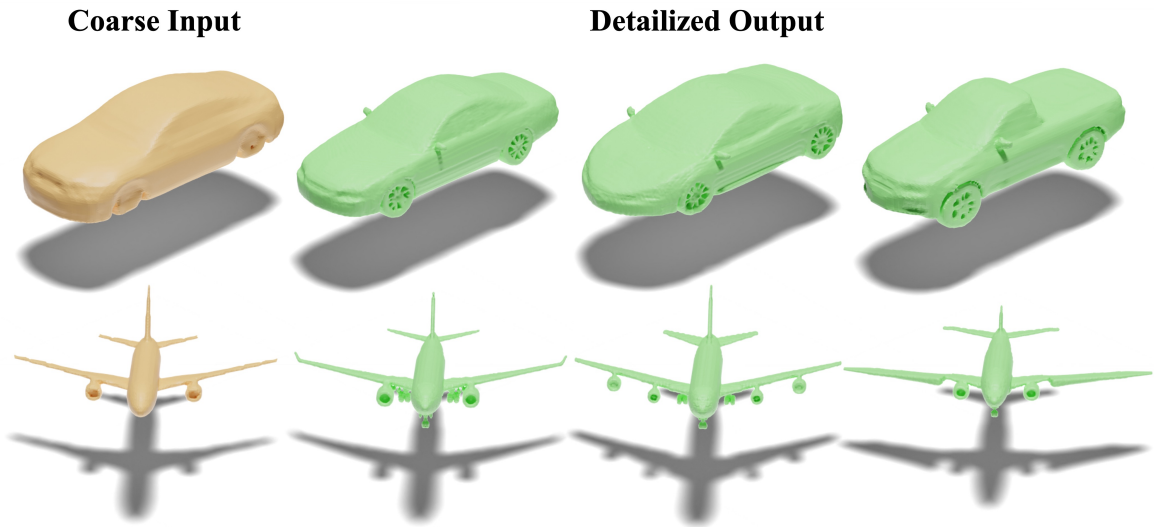


Fig. 8. **Diverse generation results.** Our method is capable of generating a diverse array of detailed results from the same coarse input, showcasing its robustness and flexibility in handling variations in 3D shape refinement.

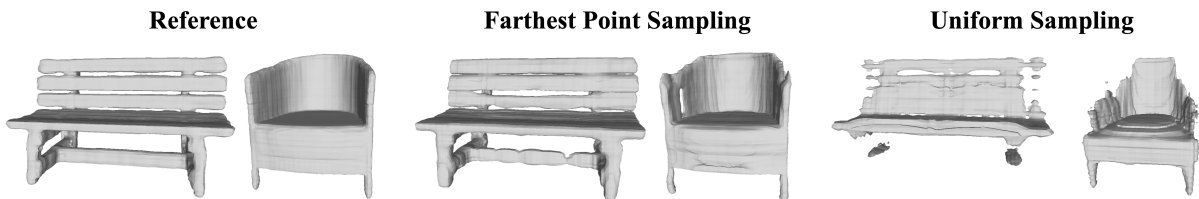


Fig. 9. **Downsampling strategy ablation.** We present the mid-Level of Detail (LOD) reconstruction results utilizing both sampling strategies, with the final-LOD reconstruction serving as a reference for comparative analysis.

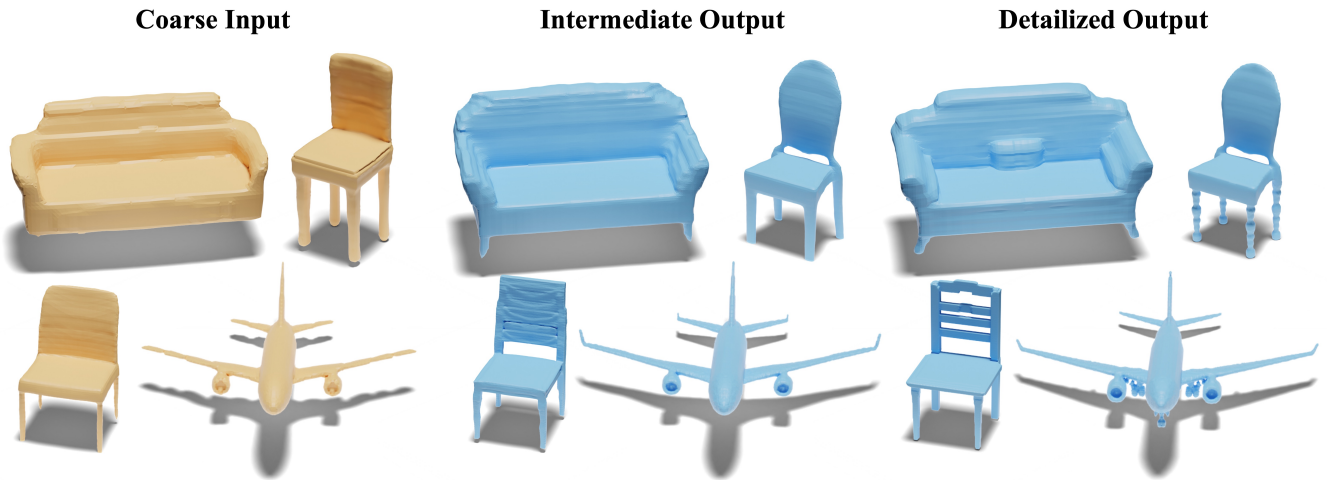


Fig. 10. **Multi-LOD detailed output.** We demonstrate the detailization capabilities of our model by showcasing the generation of meshes across various scales. This process highlights the model’s proficiency in producing detailed geometric structures from coarse to fine LODs.

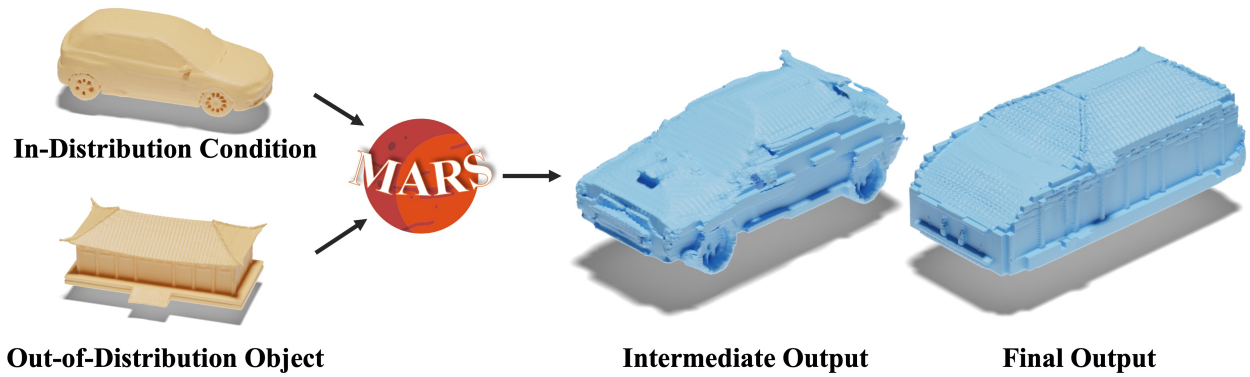


Fig. 11. **Mixing styles application.** Our model is capable of performing style-mixing by utilizing one shape as a conditioning input to detailize another shape. It underscores the model’s flexibility in integrating stylistic elements from one geometry into the detailed enhancement of another.

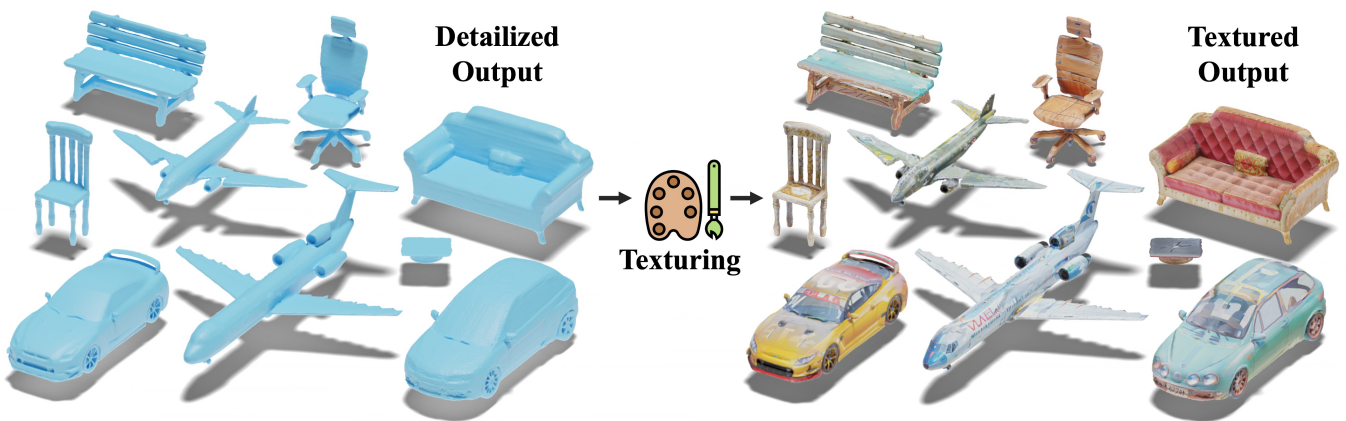


Fig. 12. **Textured results using detailed output.** We demonstrate the results of texturing the detailed output in the teaser section, showcasing the enhanced visual fidelity achieved through our proposed methodology.